ELSEVIER

Contents lists available at ScienceDirect

# **Accident Analysis and Prevention**

journal homepage: www.elsevier.com/locate/aap



# Understanding whiplash injury and prevention mechanisms using a human model of the $neck^*$

Paul C. Ivancic\*, Ming Xiao

Biomechanics Research Laboratory, Department of Orthopaedics and Rehabilitation, Yale University School of Medicine, New Haven, CT, USA

#### ARTICLE INFO

Article history:
Received 3 September 2010
Received in revised form 4 January 2011
Accepted 15 February 2011

Keywords: Whiplash Cervical spine Biomechanics Injury prevention

#### ABSTRACT

Objectives: Various models for rear crash simulation exist and each has unique advantages and limitations. Our goals were to: determine the neck load and motion responses of a human model of the neck (HUMON) during simulated rear crashes; evaluate HUMON's biofidelity via comparisons with *in vivo* data; and investigate mechanisms of whiplash injury and prevention.

Methods: HUMON, consisting of a neck specimen (n = 6) mounted to the torso of BioRID II and carrying a surrogate head and stabilized with muscle force replication, was subjected to simulated rear crashes in an energy-absorbing seat with fixed head restraint (HR) at peak sled accelerations of 9.9 g ( $\Delta V$  9.2 kph), 12.0 g ( $\Delta V$  11.4 kph), and 13.3 g ( $\Delta V$  13.4 kph). Physiologic spinal rotation ranges were determined from intact flexibility tests. Average time–history response corridors ( $\pm 1$  standard deviation) were computed for spinal motions, loads, and injury criteria.

Results: Neck loads generally increased caudally and consisted of shear, compression, and flexion moment caused by straightening of the kyphotic thoracic and lordotic lumbar curvatures, upward torso ramping, and head inertial and head/HR contact loads. Nonphysiologic rotation occurred in flexion at C7/T1 prior to head/HR contact and in extension at C6/7 and C7/T1 during head/HR contact.

Conclusions: HUMON's neck load and motion responses compared favorably with *in vivo* data. Lower cervical spine flexion—compression injuries prior to head/HR contact and extension—compression injuries during head/HR contact may be reduced by refinement of existing seatback, lapbelt, and HR designs and/or development of new injury prevention systems.

© 2011 Elsevier Ltd. All rights reserved.

# 1. Introduction

Epidemiologists estimate the total lifetime costs of fatal and nonfatal motor vehicle crashes, including medical care and lost productivity, at over \$99 billion in 2005 alone (Naumann et al., 2010). The incidence of whiplash neck injury is highest in rear crashes as compared to other crash configurations (Jakobsson et al., 2000). Recent advances in head restraint (HR) geometry and functionality and energy-absorption capability of the seat have led to reduction, but not complete elimination, of whiplash injuries (Jakobsson et al., 2008; Viano and Olsen, 2001).

To better understand whiplash injury and prevention mechanisms, rear crashes are simulated using human volunteers (McConnell et al., 1995; Ono et al., 1997), mathematical models

E-mail address: paul.ivancic@yale.edu (P.C. Ivancic).

(Himmetoglu et al., 2008), crash dummies (Siegmund et al., 2005), whole cadavers (Luan et al., 2000), isolated head/neck specimens (Ivancic et al., 2005; Kettler et al., 2004), and hybrid cadaveric/surrogate models such as human model of the neck (HUMON) (Ivancic et al., 2009). Each has unique advantages and limitations. The human volunteer studies provide occupant load and motion response corridors which are the gold standard from which other model responses may be compared, however the in vivo data do not provide injury responses. Mathematical models and rear crash test dummies are useful for parametric studies of safety system efficacy, however these models can neither be injured nor can they provide injury responses. Mathematical model output is highly dependent upon the accuracy of complex input data, including detailed spinal anatomy, muscle and ligament mechanical properties, and muscle activation patterns. In contrast, whole cadavers, isolated head/neck specimens, and hybrid cadaveric/surrogate models may be injured thus providing injury responses during simulated crashes of high severity. While these models lack active musculature, they replicate the response of an unwarned subject during a simulated

The goals of this study were to: determine the neck load and motion responses of HUMON during simulated rear crashes; eval-

<sup>★</sup> This research was supported by grant 5R01CE001257 from the Centers for Disease Control and Prevention (CDC).

<sup>\*</sup> Corresponding author at: Biomechanics Research Laboratory, Department of Orthopaedics and Rehabilitation, Yale University School of Medicine, 333 Cedar Street, P.O. Box 208071, New Haven, CT 06520-8071, USA. Tel.: +1 203 785 4052; fax: +1203 785 7069.

uate HUMON's biofidelity via comparisons with *in vivo* data; and investigate mechanisms of whiplash injury and prevention.

#### 2. Materials and methods

#### 2.1. Specimen preparation and physiologic rotation

We mounted six fresh-frozen human osteoligamentous whole cervical spine specimens (occiput-T1) in resin at the occiput and T1 vertebra (2 M, 4 F; average age 86 years; range: 79–90 years). Apart from typical age related degenerative changes, the specimens did not suffer from any disease that could have affected the osteoligamentous structures. Lightweight motion-tracking flags with 9.5 mm diameter markers were rigidly attached to each cervical vertebra (C1 through C7) and to the occipital and T1 mounts.

Physiologic spinal rotation was obtained from intact flexibility testing up to 1.5 Nm flexion and extension moments. Loads were applied incrementally in four equal steps to the occipital mount via a loading jig while the T1 mount remained fixed. The weights of the loading jig and occipital mount were counterbalanced throughout the tests. To allow for viscoelastic creep, 30 s break periods were given following each load application. After two preconditioning cycles, spinal rotation data were recorded at each load increment of the third loading cycle. The physiologic spinal rotation range was the average peak rotation +1 SD.

#### 2.2. Human model of the neck (HUMON)

HUMON (Fig. 1A) consisted of the neck specimen with its T1 mount rigidly connected to the torso of a rear impact dummy, BioRID II (Denton ATD Inc, Milan, OH, USA) (Svensson, 1993; Svensson et al., 2000), and carrying a custom anthropometric surrogate head (Ivancic et al., 2009). When mounted to the torso of BioRID II, the occipital mount and head were aligned horizontally and the average vertebral flexion angles relative to the horizontal measured by radiography were: 12.9° C1, 22.3° C2, 33.2° C3, 36.2° C4, 44.8° C5, 47.6° C6, 47.6° C7, and 40.5° T1. Inclination was defined for C1 as the angle between the horizontal and the line through the centers of the anterior and posterior tubercules and for C2 through T1 as the angle between the horizontal and the inferior endplate (line through anteroinferior and posteroinferior corners of each vertebral body). These data indicated an initial flexed posture of the subaxial cervical spine and extended posture at head/C1, as compared to the in vivo neutral posture (Descarreaux et al., 2003). The head included a six-component load cell (MC3A force/torque sensor; load capacities of Fz: 2200 N, Fy: 4400 N, and Mx: 110 Nm; Advanced Mechanical Technology, Inc., Watertown, MA) rigidly connected to the occipital mount. The head (4.6 kg mass; 0.0214 kg m<sup>2</sup> sagittal moment of inertia) had a motion tracking marker rigidly fixed to its right side at its sagittal center of mass location. The head and neck were stabilized using the compressive muscle force replication (MFR) system (Fig. 1B) (Ivancic et al., 2005). The MFR consisted of two anterior, two posterior, and bi-lateral cables originating at the head and bi-lateral cables originating at C2, C4, and C6. Each cable was connected to a separate spring with a stiffness coefficient of 4.0, 4.0 and 8.0 N/mm for the anterior, lateral, and posterior springs, respectively. The preload was 15 N in each anterior and posterior spring and 30 N in each lateral spring. With this MFR arrangement the compressive neutral posture pre-loads at each spinal level were: 120 N (head/C1, C1/2); 180 N (C2/3, C3/4); 240 N (C4/5, C5/6) and 300 N (C6/7, C7/T1). These preloads are in good agreement with the estimated in vivo spinal compression at C4/5, ranging between 122 N in relaxed posture and 1164N with maximally active neck muscles calculated using a mathematical model (Moroney et al., 1988). Our MFR sys-

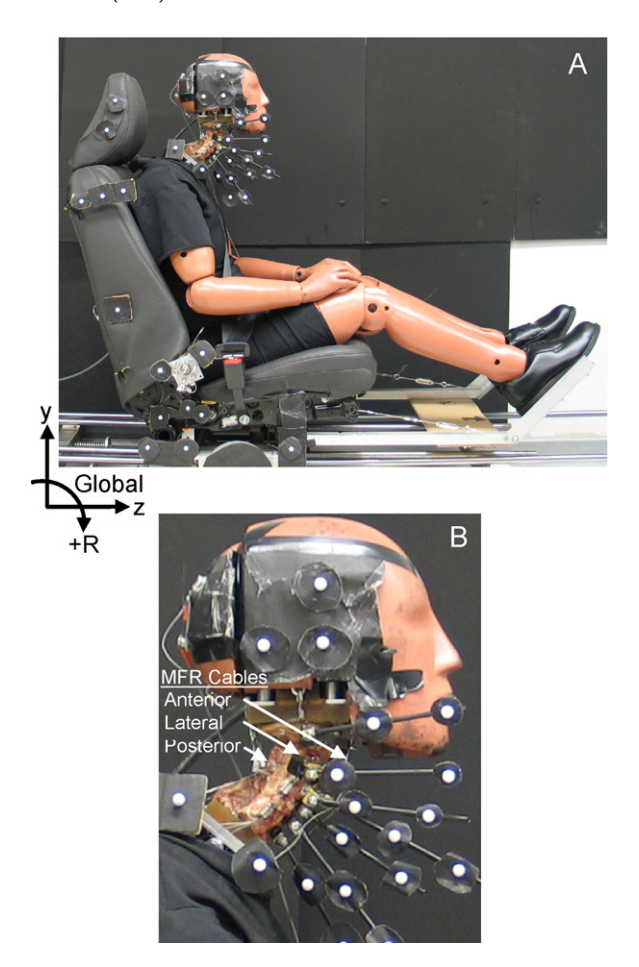


**Fig. 1.** (A) Photograph of the human model of the neck (HUMON) used to simulate rear crashes. Motion tracking flags were fixed to the head, cervical vertebrae, T1, and pelvis while an accelerometer was fixed to the sled. The global coordinate system has its *z*-axis horizontal and positive forward and *y*-axis vertical and positive upward. Rotation is positive for flexion and negative for extension. (B) HUMON's human cervical spine showing placement of muscle force replication (MFR) cables.

tem, which provides postural neck stability and passive resistance to intervertebral motions during the simulated crash, produces a high-speed kinematic response of the neck similar to *in vivo* data (Ivancic et al., 2005). No preload was applied to the anthropometric thoracic or lumbar spine regions. A motion tracking flag was rigidly fixed to the pelvis on HUMON's right side.

# 2.3. Dynamic evaluation of HUMON

We simulated rear crashes at average maximum measured horizontal sled accelerations of 9.9 g ( $\Delta V$  9.2 kph), 12.0 g ( $\Delta V$  11.4 kph), and 13.3 g ( $\Delta V$  13.4 kph). The crash apparatus consisted of an automobile seat mounted on a custom sled in which HUMON was seated in normal driving posture and secured with a seatbelt (Fig. 1A). We used the front drivers seat of a 2005 Volvo XC90 minivan with WHIPS and fixed HR (Volvo Car Corporation, Göteborg, Sweden) (Lundell et al., 1998). The energy-absorbing components of WHIPS were replaced prior to each subsequent crash (Service Kit, Part #31250443, Volvo Car Corporation, Göteborg, Sweden). A highspeed digital camera recorded the sagittal motions of the flag markers at 500 frames/s with resolution of 28.3 pixels/cm (Motion-PRO, Redlake MSAD, San Diego, CA, USA). A contact switch mounted to the back of the head determined the time of head/HR contact. A bi-axial accelerometer (50 g capacity; part no. ADXL250JQC, Analog Devices, Norwood, MA, USA) was fixed to the sled. Accelerometer and load cell data were continuously sampled at 1 kHz using an analog-to-digital converter and a personal computer. A pneumatic braking system gradually decelerated HUMON following the crash.

#### 2.4. Data analyses

We determined the average time-history response corridors ( $\pm 1$  standard deviation) for the spinal motions, loads, and injury criteria. All data were digitally filtered using a third order, dual pass, Butterworth low-pass filter at a cutoff frequency of 30 Hz.

#### 2.4.1. Spinal motions

Custom Matlab programs were used to obtain the coordinates of the flag markers with sub-pixel accuracy and to compute the spinal rotations during the crashes and throughout the flexibility tests. A cervical spine radiograph, that most closely matched average vertebral dimensions (Panjabi et al., 1991a; Panjabi et al., 1991b) and which clearly showed all vertebrae, was scaled equally in the horizontal and vertical directions and aligned accordingly and digitally superimposed on the first frame of the high-speed movie (Adobe Photoshop CS2, Version 9, San Jose, CA). We established geometric rigid body relationships between the flag marker centers and the occipital condyles and approximate centers of mass of each vertebra, C1 through T1, and pelvis. For each subsequent movie frame, translations of the occipital condyles and vertebral and pelvic centers of mass were computed and expressed in the global coordinate system using, as input, rotation data, flag marker translations, and the geometric rigid body relationships (Ivancic et al., 2006b). The global coordinate system was fixed to the ground and had its zaxis horizontal and positive forward and y-axis vertical and positive upward (Fig. 1A). Rotation is positive for flexion and negative for extension. Average (SD) system errors, as determined in separate studies were 0.00° (0.34°) for rotation (Ivancic et al., 2009) and 0.3 mm (0.2 mm) for translation (Pearson et al., 2004).

#### 2.4.2. Spinal loads

We used inverse dynamics to compute the loads at the occipital condyles and vertebral centers of mass using as input: head load cell data, head and vertebral masses and mass moments of inertia, linear and angular head and vertebral accelerations, and the aforementioned vertebral motion data (Ivancic et al., 2006a). We used vertebral mass and mass moment of inertia data from the National Library of Medicine's Visible Human Data Set (Camacho et al., 1997). The linear (horizontal and vertical) and angular accelerations of the head and vertebrae were computed in the global coordinate system by numerical double differentiation of the corresponding motion data. The vertebral loads were calculated caudally beginning from the known loads measured by the head load cell. Occipital condyle and vertebral forces were expressed in anatomic coordinate systems which were fixed to and moved with the head/vertebrae, respectively. The head and vertebral coordinate systems were aligned with the global coordinate system immediately prior to the crash. Average (SD) errors in the computed loads were  $0.5 \,\mathrm{N}\,(1.8\,\mathrm{N})$  for shear force,  $-0.1 \,\mathrm{N}\,(2.2\,\mathrm{N})$  for axial force, and 0.7 Nm (0.7 Nm) for moment (Ivancic et al., 2006a).

### 2.4.3. Cervical spine injury criteria

We computed the: neck injury criterion (NIC); neck protection criterion (Nkm); normalized neck injury criterion (Nij); and neck displacement criterion (NDC). The NIC was computed using the relative horizontal acceleration and velocity between the head and T1 centers of mass (Bostrom et al., 1996). The NDC was computed using motions of the occipital condyles relative to the T1 center of mass and was exemplified by plotting the average head/T1 rotation and axial separation/compression vs. shear (Viano and Davidsson, 2002). Nkm, a function of shear force and moment at the occipital condyles, incorporated intercept values of 845 N for anterior and

positive shear, 88.1 Nm for flexion moment, and 47.5 Nm for extension moment (Schmitt et al., 2002). Nij, a function of axial force and moment at the occipital condyles, incorporated intercept values of 6806 N for tension, 6160 N for compression, 310 Nm for flexion moment, and 125 Nm for extension moment (Eppinger et al., 1999).

#### 3. Results

Average time-history responses for spinal loads and motions appear in Fig. 2. Average duration of head/HR contact was 90 ms (116 to 206 ms) for 9.9 g, 96 ms (120 to 216 ms) for 12.0 g, and 92 ms (114 to 206 ms) for 13.3 g. The physiologic spinal rotation range, indicated by grey horizontal shading in Fig. 2F, was  $40.6^{\circ}$  flexion and  $48.9^{\circ}$  extension at head/T1 and among spinal levels was largest at the upper cervical spine (head/C1:  $8.9^{\circ}$  flexion,  $12.4^{\circ}$  extension; C1/2:  $11.6^{\circ}$  flexion,  $10.6^{\circ}$  extension) and least at C7/T1 ( $3.0^{\circ}$  flexion,  $4.6^{\circ}$  extension).

Loads at the occipital condyles and cervical vertebrae consisted of shear and axial forces coupled with sagittal moments (Fig. 2A–C). Average peak loads generally increased caudally. Prior to head/HR contact, loads consisted of anterior followed by posterior shear, compression, and flexion moment. During this time period, the highest average peak loads occurred at C7 during the 13.3 g crash reaching 13.0 N anterior shear, 97.2 N posterior shear, 617.7 N compression, and 22.6 Nm flexion moment. During head/HR contact, loads consisted of anterior shear, compression, and flexion moment increasing from the occipital condyles to C7 (85.8–151.7 N anterior shear; 39.8–240.6 N compression; 1.5–16.5 Nm flexion moment).

Average spinal and pelvic motions consisted of forward and upward translations in the global coordinate system and intervertebral rotations of flexion and extension (Fig. 2D-F). During the 13.3 g crash, the onset of forward translation began initially at the pelvis (20 ms) and then sequentially from T1 (72 ms) through the occipital condyles (78 ms). Upward translation began initially at the pelvis (46 ms) and then at the neck (60 ms). Upward translation peaks were least at the pelvis (3.1 cm) and sequentially increased from T1 (6.4 cm) to the upper cervical spine (8.3 cm). Prior to head/HR contact, head/T1 flexion was caused primarily by C6/7 and C7/T1 flexion with minimal rotation at the superior spinal levels. During head/HR contact, rotation in opposing directions throughout the neck occurred with flexion at head/C1 to C3/4 and extension at C4/5 to C7/T1, resulting in net head/T1 extension. While head/T1 rotation remained within the physiologic range, nonphysiologic rotations occurred at C6/7 and C7/T1.

Average peak NIC (16.4 m<sup>2</sup>/s<sup>2</sup>), Nkm (0.12), and Nij (0.08) occurred prior to head/HR contact (Fig. 3A–C). During this time period, NDC demonstrated head/T1 motions consisting of flexion and forward and downward translations which reversed direction during head/HR contact (Fig. 3D and E).

#### 4. Discussion

In this study, we observed distinct neck load and motion responses prior to and following head/HR contact during simulated rear crashes of HUMON seated on an energy-absorbing seat. Previously reported data obtained from simulated rear crashes of human volunteers form the gold standard from which our data may be compared. These cumulative data, in addition to findings from crash simulations of whole cadavers, provide insight into whiplash injury and prevention mechanisms.

HUMON and all other crash models have unique advantages and limitations. HUMON consists of BioRID II, a 50th percentile male dummy, with its artificial neck replaced by a human neck specimen. The present specimens, with an average age of 86 years, most likely had decreased bone mass, density, and strength as compared

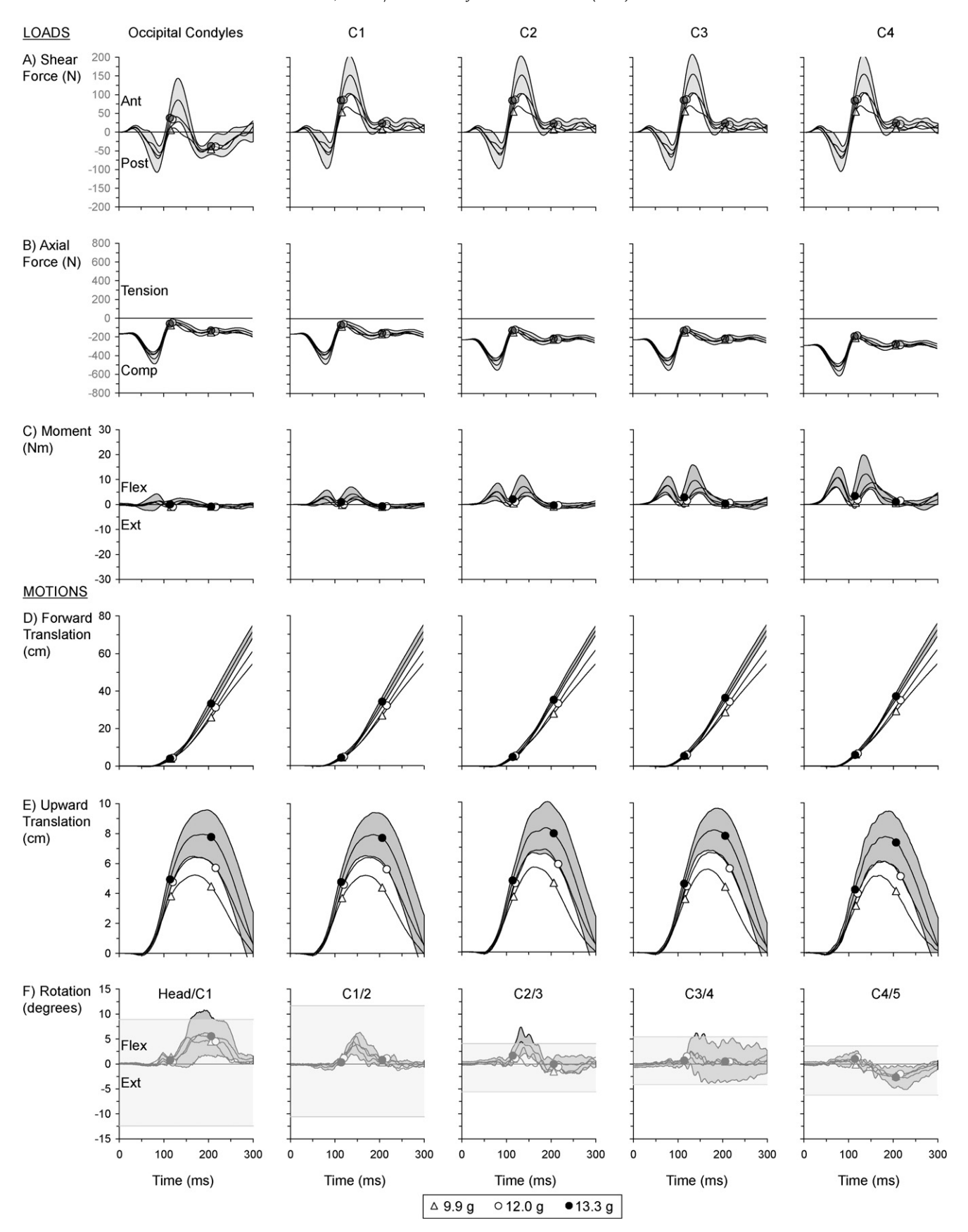


Fig. 2. Average time-history responses for spinal loads and motions. Loads at the occipital condyles and vertebrae (C1 through T1) include: (A) shear force (N): anterior (positive) and posterior (negative); (B) axial force (N): tension (positive) and compression (negative); and (C) moment (Nm): flexion (positive) and extension (negative). Forces were expressed in anatomic coordinate systems which were fixed to and moved with the head/vertebrae. Motions include: (D) forward and (E) upward translations (cm) of the occipital condyles, cervical vertebrae, T1, and pelvis in the global coordinate system; and (F) spinal rotations (°) in flexion (positive) and extension (negative). For clarity, shaded regions representing the average response  $\pm 1$  SD are shown only for the 13.3 g crash. Average onset and end of head/HR contact is indicated for each crash: 9.9 g ( $\triangle$ ), 12.0 g ( $\bigcirc$ ), and 13.3 g ( $\blacksquare$ ). The physiologic rotation range (average +1 SD) for each spinal level and head/T1 is indicated by grey horizontal shading in panel F.

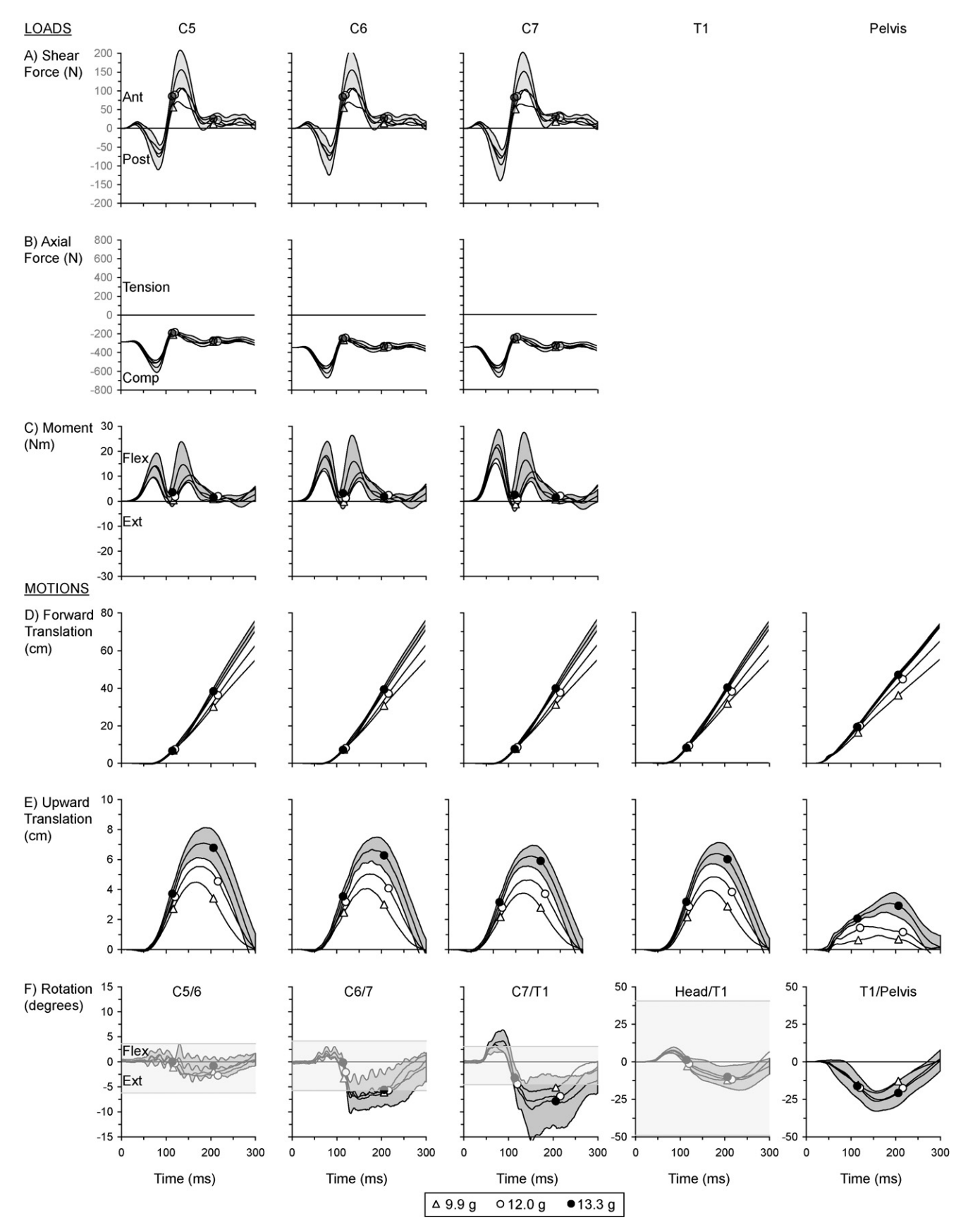
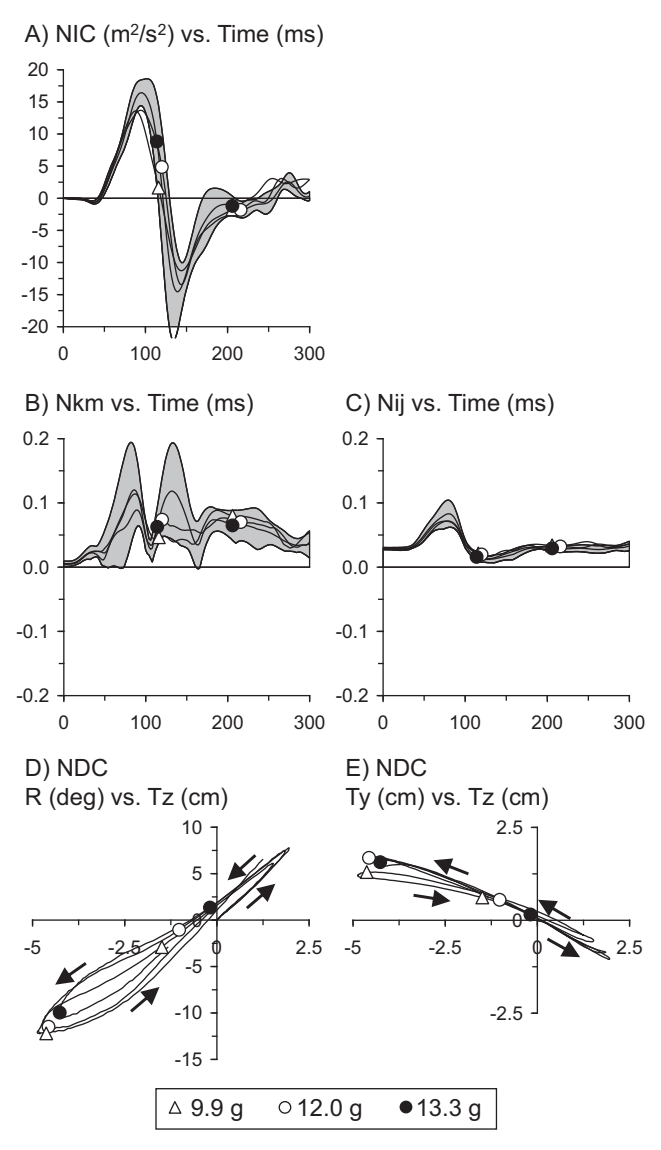


Fig. 2. (Continued).



**Fig. 3.** Average time—history responses for: (A) NIC  $(m^2/s^2)$ ; (B) Nkm; (C) Nij; (D) NDC: rotation  $(R,^\circ)$  vs. shear translation (Tz, cm); and (E) NDC: axial translation (Ty, cm) vs. shear translation (Tz, cm). For clarity, shaded regions representing the average response  $\pm 1$  SD are shown only for the 13.3 g crash in panels A–C. Average onset and end of head/HR contact is indicated for each crash: 9.9 g ( $\triangle$ ), 12.0 g ( $\bigcirc$ ), and 13.3 g ( $\blacksquare$ ). Arrows in panels D and E indicate the direction of motion beginning at time = 0 ms.

with the 50th percentile male. Thus, HUMON's neck loads imparted by head inertia and torso ramping and straightening were likely larger than those experienced by older rear crash occupants. The initial posture of the neck specimens was flexion at the subaxial cervical spine and extension at CO/1 as compared to the in vivo neutral posture (Descarreaux et al., 2003) thus indicating an initial out of position neck alignment. These cumulative factors indicated a near worst case scenario for causation of large neck loads and motions. HUMON's advantages far outweigh its limitations. Neck response to injurious loads and motions and effects of safety systems on reducing neck injuries are attainable using HUMON but not human volunteer studies. HUMON permits testing of a greater specimen sample size and the use of physiologic compressive MFR to provide postural neck stability and passive resistance to spinal motions during the crash. In contrast, intact whole cadavers are available in limited quantities at high cost and typically a nonphysiologic tensile force opposed to compressive MFR is used to support the head weight prior to the crash. Mathematical models and surrogate test dummies cannot be injured nor can they provide injury responses. In a study of simulated rear crashes using isolated head/neck specimens, Kettler et al. (2004) observed improved biofidelity of dynamic neck loads using an acceleration apparatus that allowed pre-defined T1 rotation. Isolated head/neck models, alone, are limited in that they do not permit comparisons of injury responses between anti-whiplash seats. Rear crashes of HUMON, which simulate torso/seatback interactions including thoracic spine straightening and upward torso ramping, may be used for future comparisons and optimization of anti-whiplash seat and HR systems.

Prior to head/HR contact, HUMON's neck loads consisted of anterior followed by posterior shear, compression, and flexion moment (Fig. 2A-C) while motions at C6/7 and C7/T1 in flexion caused net head/T1 flexion (Fig. 2F). These load and motion patterns are consistent with those observed during simulated rear crashes of human volunteers (Ono et al., 1997) and whole cadavers (Luan et al., 2000). During a rear crash, the seat base accelerates forward and the torso presses into the seatback due to its inertia causing seatback deflection and straightening of the kyphotic thoracic curvature and lordotic lumbar curvature (Ono et al., 1999). The pelvis and T1 vertebra translate upward and net T1/pelvis extension occurs (Fig. 2E and F). Luan et al. (2000) and Ono et al. (1997) hypothesized that neck compressive force is due to straightening of the thoracic spine and upward ramping of the torso on the seatback. These researchers observed that thoracic spine straightening caused sequential extension of the vertebrae of the lower cervical spine from inferior to superior as load transferred superiorly. Their data support our findings. Luan et al. (2000) hypothesized that the lower cervical spine was subjected to a flexion moment immediately following the crash, consistent with our findings. We observed the onset of intervertebral flexion rotation at C7/T1 (38 ms) prior to C6/7 (48 ms). Extension onset of the inferior vertebra prior to the superior vertebra caused intervertebral flexion with the lag time due to superior vertebra inertia. As the C7/T1 posterior ligaments became taut, load transferred superiorly to cause extension of the C7 vertebra resulting in C6/7 flexion. These load and motion patterns caused posterior ligament tension and anterior disc compression at C6/7 and C7/T1. Kaneoka et al. (1997) observed further intervertebral flexion at superior spinal levels up to C2/3. Our results indicate head/T1 flexion was caused primarily by C6/7 and C7/T1 flexion, with little rotation at superior spinal levels until head/HR contact. We observed nonphysiologic flexion at C7/T1 during the 13.3 g crash indicating potential tensile injury of the supraspinous, interspinous, and capsular ligaments and the ligamentum flavum and compression injury at the anterior disc. This injury potential is further supported by NIC in excess of the proposed 15 m<sup>2</sup>/s<sup>2</sup> injury threshold (Fig. 3A) at the time of peak C7/T1 flexion prior to head/HR contact.

Our data, which indicate that even modern anti-whiplash seats may not protect the lower cervical spine from flexion-compression injuries prior to head/HR contact, are supported by the findings of previous in vivo rear crash studies. McConnell et al. (1995) simulated rear crashes using human volunteers and observed that while standard HRs did not prevent potential compressive neck injury, flexible seatbacks may provide injury protection. These researchers observed that torso upward motion and thoracic spine straightening ended shortly after upward compliance permitted by the lapbelt was attained (McConnell et al., 1993). Epidemiological and biomechanical studies indicate increased whiplash injury with increased seatback rigidity and strength (Prasad et al., 1997; Strother and James, 1987). Seatbacks must be yielding to reduce whiplash injuries during low severity crashes yet rigid enough to limit rotation and achieve occupant retention during high severity crashes. High retention seats, consisting of a strong outer frame and yielding perimeter frame, allow occupant displacement into the seatback while maintaining an upright frame (Viano, 2004). We studied a modern anti-whiplash seat which absorbed crash energy by simultaneous rearward and downward translations and extension of the seatback and occupant displacement into the seatback (Lundell et al., 1998). Flexion–compression injuries of the lower cervical spine prior to head/HR contact may be reduced by simultaneous refinement of seatback and lapbelt designs.

During head/HR contact, HUMON's neck loads consisted of anterior shear, compression, and flexion moment (Fig. 2A-C) while rotation in opposing directions occurred with flexion at head/C1 to C3/4 and extension at C4/5 to C7/T1, resulting in net head/T1 extension (Fig. 2F). Some previous in vivo and whole cadaver rear crash simulations caused tensile neck forces (Luan et al., 2000; Ono et al., 1997; Siegmund et al., 2001) while others caused only compressive forces (Kaneoka et al., 1997; van den Kroonenberg et al., 1998). Previous simulated rear crashes of head/neck specimens with no HR or torso ramping caused initial tensile neck forces (Ivancic et al., 2006a). Axial neck force orientation likely depends upon multiple factors including HR position, neck muscle activity, and torso/seatback interactions including thoracic spine straightening and upward torso ramping. HUMON's head and neck were stabilized using compressive MFR. Head/T1 separation during head/HR contact, indicated by +Ty in Fig. 3E, caused increased MFR cable load thus counteracting the neck tensile force due to head inertia. Minimum neck compression occurred at the onset of head/HR contact (Fig. 2B). The present seat included a fixed HR positioned above HUMON's head center of mass (Fig. 1A) and a neck flexion moment was consistently observed during head/HR contact. Siegmund et al. (2005) found that sagittal neck moment orientation is sensitive to HR height. These researchers observed a large neck extension moment due to wrapping of the head onto the top of a low-position HR which changed to a flexion moment with a high-position HR.

We observed nonphysiologic extension at C6/7 and C7/T1 during head/HR contact indicating potential tensile injury of the anterior longitudinal ligament and anterior annular fibers and compression injury to the facet joints. Following the onset of head/HR contact, head inertial and head/HR contact loads were transferred through the neck as torso upward motion and thoracic spine straightening continued. The C7 vertebra rotated in extension more than the T1 vertebra and subsequently C6 extended more than C7 resulting in hyperextension at C6/7 and C7/T1. These motions occurred during the well documented S-shaped neck curvature (Grauer et al., 1997) as the head relative to T1 was translated rearward and upward and extended (Fig. 3D and E). No extension occurred at head/C1 or C1/2 indicating a prolonged S-shaped neck curvature as compared to previous rear crash simulations with no HR (Ivancic et al., 2005). Reversal of thoracic and lumbar spine rotations occurred prior to the end of head/HR contact and return of the original kyphotic thoracic and lordotic lumbar curvatures occurred by 300 ms. Lower cervical spine hyperextension during head/HR contact was caused by combined head loads transferred inferiorly and torso loads transferred superiorly causing shear, compression, and flexion moment. Extension-compression injuries of the lower cervical spine during head/HR contact may be reduced by simultaneous refinement of seatback, lapbelt, and HR systems.

#### 5. Conclusions

We observed distinct neck load and motion responses prior to and during head/HR contact due to simulated rear crashes of HUMON seated on an energy-absorbing seat. HUMON's neck loads consisted of shear, compression, and flexion moment. Prior to head/HR contact, neck motions consisted of flexion at the lower cervical spine, C6/7 and C7/T1, with nonphysiologic flexion at C7/T1. During head/HR contact, neck rotation in opposing direc-

tions occurred with flexion at head/C1 to C3/4 and extension at C4/5 to C7/T1, with nonphysiologic extension at C6/7 and C7/T1. Lower cervical spine flexion–compression injuries prior to head/HR contact and extension–compression injuries during head/HR contact may be reduced by simultaneous refinement of seatback, lapbelt, and HR designs and/or development of new injury prevention systems.

#### References

- Bostrom, O., Svensson, M.Y., Alsman, B., Hansson, H.A., Haland, Y., Lovsund, P., Seeman, T., Suneson, A., Salgo, A., Ortengran, T., 1996. A new neck injury criterion candidate based on injury findings in the cervical spinal ganglia after experimental neck extension trauma. In: International Research Council on the Biomechanics of Impacts, Dublin, Ireland, pp. 123–136.
- Camacho, D.L., Nightingale, R.W., Robinette, J.J., Vanguri, S.K., Coates, D.J., Myers, B.S., 1997. Experimental flexibility measurements for the development of a computational head-neck model validated for near-vertex head impact. Society of Automotive Engineers Paper no. 973345.
- Descarreaux, M., Blouin, J.S., Teasdale, N., 2003. A non-invasive technique for measurement of cervical vertebral angle: report of a preliminary study. Eur. Spine J. 12. 314–319.
- Eppinger, R., Sun, E., Bandak, F., Haffner, M., Khaewpong, N., Maltese, M., Kuppa, S.,
   Nygren, T., Takhounts, E., Tannous, R., Zhang, A., Saul, R., 1999. Development
   of Improved Injury Criteria for Assessment of Advanced Automotive Restraint
   Systems II. National Highway Traffic Safety Administration, Department of
   Transportation, Washington, DC.
- Grauer, J.N., Panjabi, M.M., Cholewicki, J., Nibu, K., Dvorak, J., 1997. Whiplash produces an S-shaped curvature of the neck with hyperextension at lower levels. Spine 22, 2489–2494.
- Himmetoglu, S., Acar, M., Bouazza-Marouf, K., Taylor, A.J., 2008. Energy-absorbing car seat designs for reducing whiplash. Traffic Inj. Prev. 9, 583–591.
- Ivancic, P.C., Panjabi, M.M., Ito, S., 2006a. Cervical spine loads and intervertebral motions during whiplash. Traffic Inj. Prev. 7, 389–399.
- Ivancic, P.C., Panjabi, M.M., Ito, S., Cripton, P.A., Wang, J.L., 2005. Biofidelic whole cervical spine model with muscle force replication for whiplash simulation. Eur. Spine J. 14, 346–355.
- Ivancic, P.C., Sha, D., Panjabi, M.M., 2009. Whiplash injury prevention with active head restraint. Clin. Biomech. (Bristol, Avon) 24, 699–707.
- Ivancic, P.C., Wang, J.L., Panjabi, M.M., 2006b. Calculation of dynamic spinal ligament deformation. Traffic Inj. Prev. 7, 81–87.
- Jakobsson, L., Isaksson-Hellman, I., Lindman, M., 2008. WHIPS (Volvo cars' whiplash protection system)—the development and real-world performance. Traffic Inj. Prev. 9, 600–605.
- Jakobsson, L., Lundell, B., Norin, H., Isaksson-Hellman, I., 2000. WHIPS—Volvo's whiplash protection study. Accid. Anal. Prev. 32, 307–319.
- Kaneoka, K., Ono, K., Inami, S., Yokoi, N., Hayashi, K., 1997. Human cervical spine kinematics during whiplash loading. In: International Conference on New Frontiers in Biomechanical Engineering, Tokyo, Japan, pp. 265–268.
- Kettler, A., Schmitt, H., Simon, U., Hartwig, E., Kinzl, L., Claes, L., Wilke, H.J., 2004. A new acceleration apparatus for the study of whiplash with human cadaveric cervical spine specimens. J. Biomech. 37, 1607–1613.
- Luan, F., Yang, K.H., Deng, B., Begeman, P.C., Tashman, S., King, A.I., 2000. Qualitative analysis of neck kinematics during low-speed rear-end impact. Clin. Biomech. 15, 649–657.
- Lundell, B., Jakobsson, J., Alfredsson, B., Lindstrom, M., Simonsson, L., 1998. The WHIPS seat—a car seat for improved protection against neck injuries in rear end impacts,. In: 16th International Technical Conference on the Enhanced Safety of Vehicles, Windsor, Ontario, Canada (Paper no. 98-57-0-08).
- McConnell, W.E., Howard, R.P., Guzman, H.M., Bomar, J.B., Raddin, J.H., Benedict, J.V., Smith, H.L., Hatsell, C.P., 1993. Analysis of human test subject kinematic responses to low velocity rear end impacts. Society of Automotive Engineers Paper no. 930889.
- McConnell, W.E., Howard, R.P., Poppel, J.V., Krause, R., Guzman, H.M., Bomar, J.B., Raddin, J.H., Benedict, J.V., Hatsell, C.P., 1995. Human head and neck kinematics after low velocity rear-end impacts—understanding "whiplash". Society of Automotive Engineers Paper no. 952724.
- Moroney, S.P., Schultz, A.B., Miller, J.A., 1988. Analysis and measurement of neck loads. J. Orthop. Res. 6, 713–720.
- Naumann, R.B., Dellinger, A.M., Zaloshnja, E., Lawrence, B.A., Miller, T.R., 2010. Incidence and total lifetime costs of motor vehicle-related fatal and nonfatal injury by road user type, United States, 2005. Traffic Inj. Prev. 11, 353–360.
- Ono, K., Inami, S., Kaneoka, K., Gotou, T., Kisanuki, Y., Sakuma, S., Miki, K., 1999. Relationship between localized spine deformation and cervical vertebral motions for low speed rear impacts using human volunteers. In: Proceedings of the IRCOBI Conference, Sitges, Spain.
- Ono, K., Kaneoka, K., Wittek, A., Kajzer, J., 1997. Cervical injury mechanism based on the analysis of human cervical vertebral motion and head-neck-torso kinematics during low speed rear impacts. Society of Automotive Engineers Paper no. 973340.
- Panjabi, M.M., Duranceau, J., Goel, V., Oxland, T., Takata, K., 1991a. Cervical human vertebrae. Quantitative three-dimensional anatomy of the middle and lower regions. Spine 16, 861–869.

- Panjabi, M.M., Oxland, T.R., Parks, E.H., 1991b. Quantitative anatomy of cervical spine ligaments. Part II. Middle and lower cervical spine. J. Spinal Disord. 4, 277–285.
- Pearson, A.M., Ivancic, P.C., Ito, S., Panjabi, M.M., 2004. Facet joint kinematics and injury mechanisms during simulated whiplash. Spine 29, 390–397.
- Prasad, P., Kim, A., Weerappuli, D.P.V., Roberts, V., Schneider, D., 1997. Relationships between passenger-car seat back strength and occupant injury severity in rearend collisions: field and laboratory studies. Society of Automotive Engineers Paper no. 973343.
- Schmit, K.-U., Muser, M.H., Walz, F.H., Niederer, P.F., 2002. Nkm—a proposal for a neck protection criterion for low-speed rear-end impacts. Traffic Inj. Prev. 3, 117–126.
- Siegmund, G.P., Heinrichs, B.E., Chimich, D.D., Lawrence, J., 2005. Variability in vehicle and dummy responses in rear-end collisions. Traffic Inj. Prev. 6, 267–277.
- Siegmund, G.P., Heinrichs, B.E., Lawrence, J.M., Philippens, M., 2001. Kinetic and kinematic responses of the RID2a, Hybrid III and human volunteers in low-speed rear-end collisions. Society of Automotive Engineers Paper no. 2001-22-0011.
- Strother, C.E., James, M.B., 1987. Evaluation of seat back strength and seat belt effectiveness in rear end impacts. Society of Automotive Engineers Paper no. 872214

- Svensson, M.Y., 1993. Neck injuries in rear end car collisions—sites and biomechanical causes of the injuries, test methods and preventative measures. Ph.D. thesis, Chalmers University of Technology, Sweden.
- Svensson, M.Y., Bostrom, O., Davidsson, J., Hansson, H.A., Haland, Y., Lovsund, P., Suneson, A., Saljo, A., 2000. Neck injuries in car collisions—a review covering a possible injury mechanism and the development of a new rear-impact dummy. Accid. Anal. Prev. 32, 167–175.
- van den Kroonenberg, A., Philippens, M., Cappon, H., Wismans, J., Hell, W., Langwieder, K., 1998. Human head-neck response during low-speed rear end impacts. Society of Automotive Engineers Paper no. 983158.
- Viano, D.C. 2004. The debate between stiff and yielding seats. Society of Automotive Engineers, Warrendale, PA. Product code: PT-106.
- Viano, D.C., Davidsson, J., 2002. Neck displacements of volunteers. BioRID P3 and Hybrid III in rear impacts: implications to whiplash assessment by a neck displacement criterion (NDC). Traffic Inj. Prev. 3, 105–116.
- Viano, D.C., Olsen, S., 2001. The effectiveness of active head restraint in preventing whiplash. J. Trauma 51, 959–969.